

Phase Transition and Relaxor Behaviors in the Lead Magnesium Niobate–based Ferroelectrics

Y. J. KIM¹ and J. H. LEE²

¹*Unisontech, Cheonan 330-210*

²*Department of Applied Physics, Dankook University, Yongin 448-701*

(Received March 3, 2008)

Dielectric and pyroelectric properties of relaxor ferroelectric in the PMN-PT solid solution series have been investigated. Features of the diffuse phase transition in PMN-PT system, typical relaxor ferroelectric materials, were studied as a function of temperature and frequency. The transition temperature of the ceramics with PT~0.325 did not depend on the measuring frequency. This can best realized in a relatively random environment that apparently is provided by PMN-rich complex perovskites, including those containing Pb. The composition with PT>0.35 show the characteristics of a normal single phase ferroelectric material. Thus the studies revealed that the morphotropic phase boundary in the PMN-PT system is in the vicinity of PT~0.3 and it has a small curvature and as a result the compositions near the morphotropic phase boundary show two phase transitions, rhombohedral→tetragonal→cubic, when the samples are heated up to higher temperature. The best optimum compositions are observed near the morphotropic phase boundary.

Keywords: relaxor ferroelectrics, diffuse phase transition, frequency dispersion, Curie range

I. Introduction

Materials with the perovskite structure ABO_3 , such as $BaTiO_3$ and $PbTiO_3$, represent an important family of ferroelectrics[1]. The perovskite structure has a three dimensional net of corner sharing $[TiO_6]$ octahedra with Sr^{2+} ions in the twelve fold cavities in between the polyhedra, see Fig. 1.

Ceramics in the $Pb(Mg_{1/3}Nb_{2/3})O_3$ - $PbTiO_3$ (PMN-PT) system have important piezoelectric and electrostrictive properties. The addition of PT in PMN shifts the temperature of dielectric maximum to higher temperature. A variety of properties are possible in the PMN-PT system by simply changing the PMN and PT ratio[2].

Ordering of the B-site cations in complex perovskites occurs providing there exists a large interaction energy between neighboring cations. This interaction is based

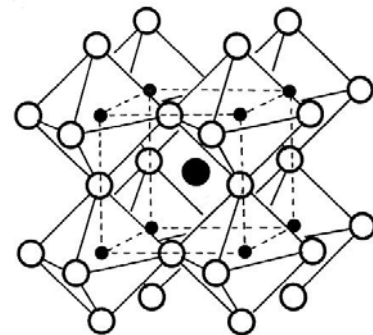


Fig. 1. Outline of the ideal cubic ABO_3 perovskite structure.

* [전자우편] yjkim80@dankook.ac.kr

on valence and ionic radii differences between the respective B' and B'' cations[3]. The structure is pseudocubic with space group Pm3m at room temperature, with no evidence of long-range ordering of the dissimilar B-site cation in the ABO₃ perovskite structure. This disorder in the B-site cation is believed to be relaxor type behavior in such materials. Though the Curie temperature or better yet, Curie range of PMN is well below room temperature, it can be easily shifted upward with PT additions, a "normal" or ordered ferroelectric compound which has a transition at 490°C. It has been reported that a morphotropic phase boundary (MPB) exists in the solid solution system PMN-PT near PT~0.4, separating rhombohedral phase and tetragonal phases[4]. As observed in other systems such as PbZrO₃-PbTiO₃ and Pb(Mg_{1/3}Ta_{2/3})O₃-PbTiO₃, anomalously large dielectric and piezoelectric properties are observed for compositions lying near the MPB[5, 6]. A systematic study of relaxor behaviors in MPB compositions in the PMN-PT system is described in this paper.

II. Experimental procedure

Ceramic samples across the PMN-PT series were prepared using the columbite precursor method as described by Swartz and Shrout[7]. X-ray diffraction patterns obtained on a laboratory diffractometer with

CuK α radiation confirmed the formation of perovskite phases with no evidence of any impurities. The dielectric properties were measured with an HP multi-frequency LCR meter (HP4275A), an environment chamber, and control unit and its interface. The pyroelectric current were measured by the static Byer-Roundy method as the samples were heated, again at a rate of 4°C/min, though the phase transition region[8].

III. Results and discussion

X-ray diffractometer was used to examine the formation of pyrochlore phase on the component surfaces. The relative amounts of the pyrochlore and perovskite phases were determined by measuring the major x-ray peak intensities for the perovskite and pyrochlore phases [(110) and (222)], respectively. For all compositions the amount of perovskite phase is 100% for 1250°C firing. In the ideal cubic the cell axis, a is geometrically related to the ionic radii (r_A , r_B , and r_O) as described in Eq. (1):

$$a = \sqrt{2}(r_A + r_B) = 2(r_B + r_O) \quad (1)$$

The ratio of all two expressions for the cell length is called the Goldschmidt's tolerance factor t and allows us to estimate the degree of distortion. It is

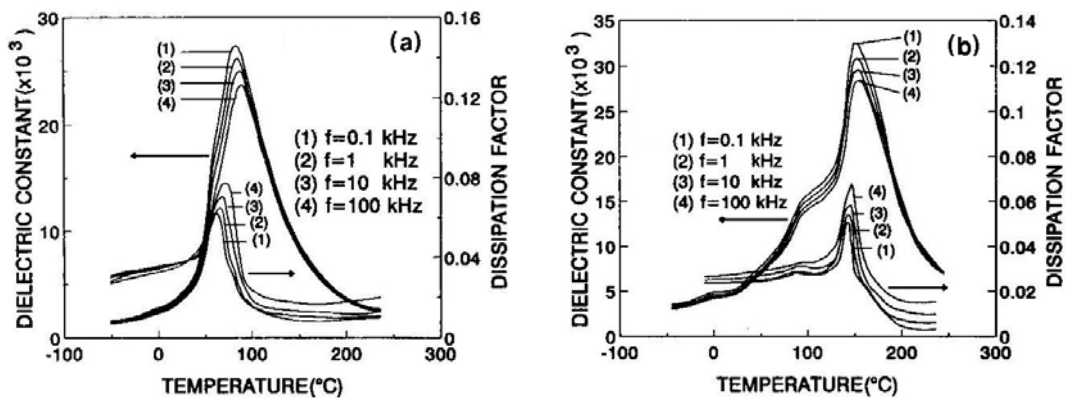


Fig. 2. Dielectric constant and dissipation factor vs temperature and frequency for (a) 0.8PMN-0.2PT and (b) 0.7PMN-0.3PT.

based on radii i.e. purely ionic bonding is assumed, but can be regarded as an indication for compounds with a high degree of ionic bonding; it is described in Eq. (2)

$$t = \frac{(r_A + r_B)}{\sqrt{2}(r_A + r_B)} \quad (2)$$

The perovskite PMN-PT has $0.891 < t < 0.894$, $r_A = 1.20 \text{ \AA}$, $r_B = 0.85 \text{ \AA}$, and $r_O = 1.40 \text{ \AA}$. If the A ion is smaller than the ideal value then t becomes smaller than 1. As a result the $[\text{BO}_6]$ octahedra will tilt in order to fill space. However, the cubic structure occurs if $0.89 < t < 1$. Lower values of t will lower the symmetry of the crystal structure.

Fig. 2(a, b) shows typical plot of the dielectric constant at various frequencies (0.1 to 100 kHz) for compositions 0.8PMN-0.2PT and 0.7PMN-0.3PT. With increasing frequency the dielectric constant decreases in magnitude and the maxima shifts to higher temperature, while for the dissipation factor, maxima decreases with an increase in frequency. They demonstrate the typical dielectric behavior of relaxor ferroelectrics[9, 10]. At high temperatures the temperature dependence of the dielectric constant is much stronger than that for the Debye medium. It was found that the temperature dependence of the dielectric constant for relaxor ferroelectrics at temperatures much higher than T_m obeys the following relation[11]:

$$K_H(T) = \exp(\alpha - \beta T) \quad (3)$$

where α and β are the constants, T is the temperature in Kelvin, and $K_H(T)$ is the measured dielectric constant at high temperatures. Fitting the measured results with Eq. (3), we get the values of both parameters $\alpha(15.45)$ and $\beta(0.017 \text{ K}^{-1})$ for 0.7PMN-0.3PT solid solutions. If the temperature is much lower than T_m , it was found that the frequency dependence of the dielectric constant can be described with the following relation[12]:

$$K_L(\omega, T) = K_\infty + A(T)(\ln\omega_o - \ln\omega) \quad (4)$$

where K_∞ is the dielectric constant at the infinite frequency, ω_o is the relaxation frequency of a polar unit cell that is independent of the temperature, $K_L(\omega, T)$ is the measured dielectric constant at temperature (T) and frequency (ω in Hz), and $A(T)$ is an intrinsic parameter of the material[13]. Thus, it should be nearly independent of the temperature as the relaxor ferroelectrics does not show any observable phase transition. Higher dielectric constant of the samples reflects of good stoichiometry[14]. The frequency dependencies of the dielectric responses, both real and imaginary, are illustrated in Fig. 2. It can be seen that a frequency reduces the dielectric constant, suppresses the frequency dispersion, and increases the temperature of the dielectric maximum. The frequency dependence of the temperature of the dielectric constant maximum can be modeled using the Vogel-Fulcher relationship given in Eq. (5)

$$\omega = f_o \exp\left(\frac{-E_a}{k(T_m - T_f)}\right) \quad (5)$$

where f_o is the Debye frequency, E_a is the activation energy, T_m is the temperature of the dielectric constant maximum, and T_f is the freezing temperature[15]. The glassy nature of relaxor in the unelectrified state probably arises due to the random dipole fields between cluster moments. If the dispersion in the local dipole field is of the same order as the mean local field, then the macroscopic system may try to partially order the cluster moments. Vugemeister have proposed a dipole interaction theory for strongly polarizable solids with soft phonon modes[16]. The correlation length has been found to saturate near freezing at 200 \AA , and the correlation radius may be approximated as 100 \AA . This indicates that relaxors are not ideal dipole glasses, but have some tendency towards ferroelectric ordering of the cluster moments. The implication is that relaxors freeze into configurations which have a texture on the

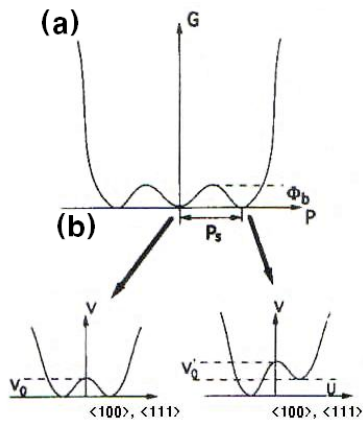


Fig. 3. (a) Free energy vs polarization in the phenomenological theory. (b) Local atomic potential along a line through two off-centered B-sites[18].

nanometer scale and that this texture is the "precursor" to long range polar order of a macrodomain state[17].

For Pb-containing perovskites, the activation barrier is dictated by a strong Pb-O-B' coupling that must be broken in order to render the material relaxant. This can be achieved by substitution of Pb^{2+} cation on the A-site of by the use of an oversized B' cation to attract Pb^{2+} cation away from the undersized B" cation[19]. In the phenomenological theory of ferroelectricity, there exists an energy barrier Φ_b between the unpolarized and polarized state at the first order phase transition temperature T_C . This is schematically depicted in Fig. 3. On an atomic level, ferroelectrically active B cations in most, if not all, ferroelectric perovskites occupy off-centered sites even at temperatures well above T_C . In the polarized state, the energy degeneracy of bifurcated state is broken by the Lorentz field in the polarized region. The relaxor behavior that shows both temperature diffuseness and frequency dispersion is possible only if hopping barrier is sufficiently small and broadly distributed. In this connection, the dielectric response of relaxors is not unlike that exhibited by many amorphous materials which contain an appreciable number of weaker/stronger bonds, lone-pair electrons, etc., which

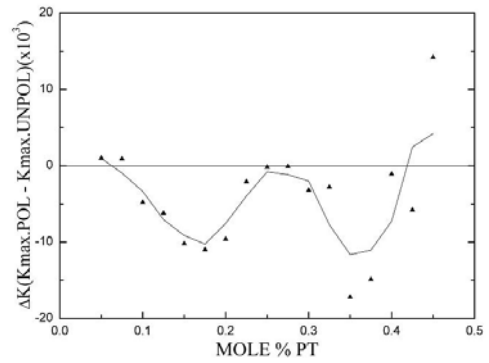


Fig. 4. The difference between maximum dielectric constants of polarized and unpolarized samples PMN-PT system as a function of mole% PT.

are though to give rise to low-lying excitations of correlated polarized states[20].

Compositions containing 0 to 0.325 mole% PT showed the stronger frequency dispersion. For ferroelectrics with a DPT, the law $1/K \approx (T - T_o)^2$ has been shown to hold over a wide temperature range instead of the normal Curie Weiss law. If the local Curie temperature distribution is Gaussian, the reciprocal dielectric constant can be written in the form

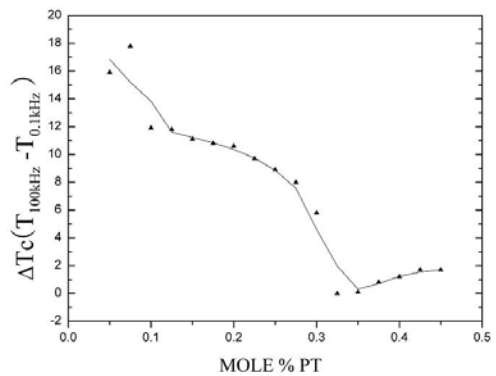


Fig. 5. A plot of ΔT_c in the PMN-PT system as a function of mole% PT.

$$\frac{1}{K} = \frac{1}{K_m} + \frac{(T - T_o)^2}{2K_m \delta^2} \quad (6)$$

Here δ is diffuseness parameter. For PMN-PT compositions, from the slope of plot $1/K$ vs $(T - T_o)^2$, the values of δ were calculated. The value of δ showed an

increase with the amount of PMN and was highest for compositions with < 0.325 PT, indicating a broadened phase transition for these compositions.

The difference between maximum dielectric constants of poled and unpoled ceramic samples are observed as shown in Fig. 4. The results have shown that the effect of polarized and unpolarized samples does not exhibit at the composition PT \sim 0.275. For these compositions there are possible poling directions over a wide temperature range. This explains why the spontaneous polarization, dielectric and piezoelectric constants are largest near the MPB. A plot of ΔT_C as a function of mole fraction of PT is shown in Fig. 5. The transition temperature of the ceramics with PT \sim 0.325 did not depend on the measuring frequency. However, plot of the transition temperature as a function of mole fraction of PT showed an anomaly at the composition PT=0.2 and 0.3 as shown in Fig. 6. Especially, at PT=0.275 \sim 0.325, it is observed that two peaks are existed in the dielectric constant versus temperature measurements as shown in Fig. 2. The first peak of low temperature anomaly may

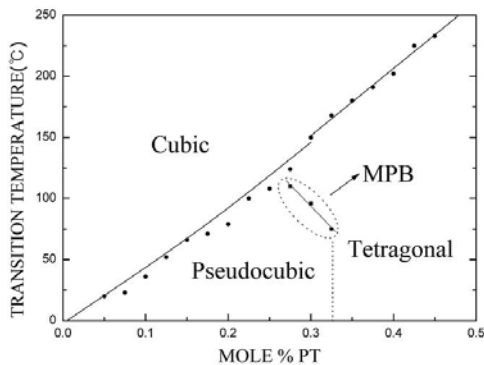


Fig. 6. Phase diagram of PMN-PT system plotted from the dielectric data. correspond to the transition from rhombohedral to tetragonal phase, and the second or high temperature peak may correspond to the transition from tetragonal to the cubic phase.

Thus both the typical dielectric and pyroelectric data (Fig. 7) indicated the presence of a second phase transition in the composition PT=0.325 in the MPB.

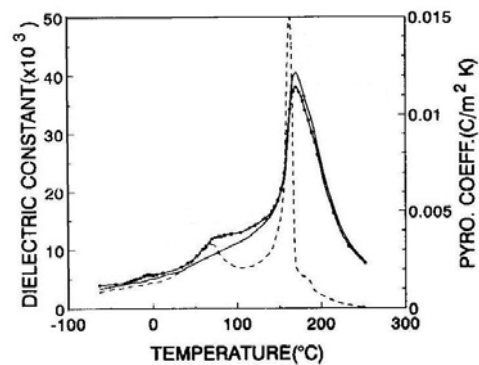


Fig. 7. The typical dielectric and pyroelectric data for 0.675PMN-0.325PT composition at 1kHz.

In most cases like in the dielectric data, two major anomalies corresponding to the phase transitions, rhombohedral \rightarrow tetragonal \rightarrow cubic, were observed. It is clear that the MPB has some curvature at composition around 0.7PMN-0.3PT.

The selected (002) or (200) diffraction patterns of PMN-PT system at room temperature are given in Fig. 8. It can be seen that at room temperatures, all the samples exhibit a single (002) or (200) reflection peak, in agreement with the perovskite cubic symmetry of the PMN-PT system. The diffraction profiles around the pseudocubic (002) and (200) diffraction peaks from PMN-PT are shown in Fig. 8(a) and (b), respectively. In each case, the observed diffraction peaks show no evidence of phase coexistence. However, this situation is very similar to that observed in the rhombohedral phase of PZT, in which a large degree of intrinsic disorder is known to exist due to the existence of local displacements of monoclinic type even though the long-range structure is rhombohedral[21, 22]. Pure PMN basically shows a single (002) peak except for a weak diffuse kink that occurs at $2\theta = 42.84^\circ$. The (200) reflection of PMN-PT exhibits a clear split at room temperatures with a narrow line width. The lower row in Fig. 8 shows the (002) reflection of PMN-PT that clearly splits into two peaks located at $2\theta = 43.87^\circ$ and 43.99° with an intensity ratio of about 1:2, as expected for a pure rhombohedral

phase. The splitting of the (200) or (002) reflection in PMN-PT indicated the formation of a rhombohedral phase at low temperatures. The MPB compositions gave considerably more complicated diffraction patterns, as can be seen in Fig. 8(c) and (d) for the 0.685PMN - 0.315PT and 0.68PMN - 0.32PT samples. From a detailed analysis of the peak positions and intensities of the fitted profiles, it was possible to identify a monoclinic phase in PMN-rich compositions, similar to that reported by Kiat and Singh[23, 24]. For example, in the case of 0.69PMN - 0.31PT it can be seen in Fig. 8(b) that the profiles of the pseudocubic (002) and (200) reflections are distinctly different from those of 0.7PMN-0.3PT shown in Fig. 8(a). Various possibilities were considered to explain the observed peak positions and intensities of

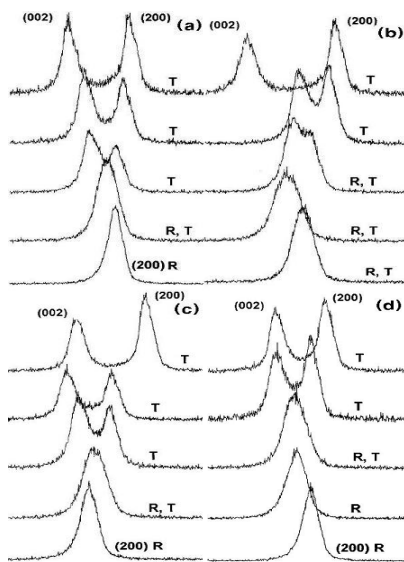


Fig. 8. X-ray diffraction patterns of PMN-PT system for (a) 0.3PT, (b) 0.31PT, (c) 0.315PT, and (d) 0.32PT.

0.69PMN-0.31PT; in particular the lower-symmetry phases previously found in this and related systems, i.e., rhombohedral and tetragonal.

IV. Conclusions

Compositions with $PT=0.10\sim 0.45$, sintered at 1250°C , showed 100% perovskite phase. The dielectric

and pyroelectric constant were found to improve with increasing sintering temperature up to 1250°C . The largest dielectric constants are found at the composition $x\sim 0.325\text{PT}$. Anomaly in the plot of the transition temperature versus mole fraction of PT was observed at the composition $PT=0.275\sim 0.325$. Maximum peak value to the pyroelectric coefficient was observed for $PT\sim 0.325$. The pyroelectric coefficient versus temperature plots showed two anomalies similar to those of dielectric data. This suggests the possibility of the curvature in the MPB in the PMN-PT system. Maximum values of the spontaneous polarization was observed for $PT\sim 0.3$. It has been shown in the present study that ferroelectric solid solution of PMN-PT with compositions close to MPB exhibit the high dielectric constant and superior pyroelectric properties. Based on the present dielectric and pyroelectric studies the MPB in the system PMN-PT possibly exists at $PT=0.275\sim 0.325$. The best optimum compositions are observed near MPB. It is important to note that the solid solutions show broadening of all phase transitions and consequently, in a certain temperature range, there can exist a paraelectric and the two ferroelectric phases (rhombohedral-tetragonal).

References

- [1] H. Gui, X. Zhang and B. Gu, *J. Phys.: Condens. Matter* **8**, 1491 (1996).
- [2] S. W. Choi, T. R. ShROUT, S. J. Jang, and A. S. Bhalla, *Mater. Lett.* **8**, 253 (1989).
- [3] S. J. Jang, Ph. D. Thesis, The Pennsylvania State University (1979).
- [4] W. Wersing, *Ferroelectrics* **7**, 163 (1974).
- [5] L. Hahn, K. Uchino, and S. Nomura, *Jpn. J. Appl. Phys.* **1**, 637 (1978).
- [6] Y. J. Kim and S. W. Choi, *Ferroelectrics* **108**, 241 (1990).
- [7] S. L. Swartz and T. R. ShROUT, *Mat. Res. Bull.* **17**,

- 1245 (1982).
- [8] R. L. Byer and C. B. Roundy, *Ferroelectrics* **3**, 333 (1972).
- [9] L. E. Cross, *Ferroelectrics* **76**, 241(1987);151, 305 (1994).
- [10] Z. Y. Cheng, R. S. Katiyar, X. Yao, and A. Guo, *Phys. Rev.* **B55**, 8165 (1997).
- [11] Z. Y. Cheng, L. Y. Zhang, and X. Yao, *J. Appl. Phys.* **79**, 8625 (1996) ;80, 5518 (1996).
- [12] Z. Y. Cheng, R. S. Katiyar, X. Yao, and A. Guo, *Phys. Rev.* **B55**, 8165 (1997).
- [13] Z. Y. Cheng, R. S. Katiyar, X. Yao, and Z. L. Wang, *Philos. Mag.* **B75**, 257 (1998).
- [14] F. Chu, I. M. Reaney, and N. Setter, *J. Am. Ceram. Soc.* **78**, 1947 (1995).
- [15] D. Viehland, S. J. Jang, L. E. Cross, and M. Wuttig, *J. Appl. Phys.* **68**, 2916 (1990).
- [16] B. Vugemeister and M. Glinchuck, *Sov. Phys. JETP* **52**, 482 (1980).
- [17] D. Viehland, S. J. Jang, and L. E. Cross, *J. Appl. Phys.* **69**(1), 414 (1991).
- [18] V. E. Zubkus and S. Lapinskas, *J. Phys.: Condens. Matter* **2**, 1753 (1990).
- [19] I. W. Chen, P. Li, and Y. Wang, *J. Phys. Chem. Solids* **57**(10), 1525 (1996).
- [20] K. L. Nagi, A. K. Jonscher, and C. T. White, *Nature* **277**, 185 (1979).
- [21] B. Noheda, D. E. Cox, G. Shirane, J. Gao, and Z. G. Ye, *Phys. Rev.* **B66**, 051104 (2002).
- [22] D. L. Corker, A. M. Glazer, R. W. Whatmore, A. Stallard, and F. Fauth, *J. Phys.: Condens. Matter* **1**, 6251 (1998).
- [23] J. M. Kiat, Y. Uesu, B. Dkhil, M. Matsuda, C. Malibert, and G. Calvarin, *Phys. Rev.* **B65**, 064106 (2002).
- [24] A. K. Singh and D. Pandey, *J. Phys.: Condens. Matter* **13**, L931 (2001).

Pb(Mg_{1/3}Nb_{2/3})O₃-based 강유전체의 상전이 및 완화특성

김연중¹ · 이주호²

¹유니슨테크, 천안 330-210

²단국대학교 응용물리학과, 용인 448-701

(2008년 3월 3일 받음)

PMN계 강유전체의 MPB 조성과 공존영역의 확산성을 이해하기 위해 유전 및 초전 특성을 분석하였다. PMN-PT계는 완만한 상전이를 보였으며, 이는 하나의 상유전과 2개의 강유전상이 공존함을 의미한다. 즉, 0.7PMN-0.3PT 조성 부근에서 능면정계와 정방정계의 공존 영역인 조성변태 상경계를 확인하였으며, 이들 조성은 연속적으로 능면정계→정방정계→입방정계로 상전이를 하였다. PT>0.325인 조성들은 측정된 진동수 범위에서 진동수 의존성을 보이지 않는 단일상의 강유전 특성을 보였으며, PMN>0.7인 조성들은 큰 진동수 의존성과 확산상전이의 전형적인 완화형 강유전 특성을 보였다. PMN-PT계의 조성변태 상경계 조성들은 우수한 유전 및 초전특성을 나타내었다.

주제어: 완화형 강유전체, 확산상전이, 진동수 분산특성, Curie 범위

* [E-mail] : yjkim80@dankook.ac.kr